https://doi.org/10.1038/s41586-018-0210-3

An Early Cretaceous eutherian and the placental–marsupial dichotomy

Shundong Bi[1,2,3]*, Xiaoting Zheng[4,5], Xiaoli Wang[4,5]*, Natalie E. Cignetti[2], Shiling Yang[6,7] & John R. Wible[3]*

Molecular estimates of the divergence of placental and marsupial mammals and their broader clades (Eutheria and Metatheria, respectively) fall primarily in the Jurassic period. Supporting these estimates, *Juramaia*—the oldest purported eutherian—is from the early Late Jurassic (160 million years ago) of northeastern China. *Sinodelphys*—the oldest purported metatherian—is from the same geographic area but is 35 million years younger, from the Jehol biota. Here we report a new Jehol eutherian, *Ambolestes zhoui*, with a nearly complete skeleton that preserves anatomical details that are unknown from contemporaneous mammals, including the ectotympanic and hyoid apparatus. This new fossil demonstrates that *Sinodelphys* is a eutherian, and that postcranial differences between *Sinodelphys* and the Jehol eutherian *Eomaia*—previously thought to indicate separate invasions of a scansorial niche by eutherians and metatherians—are instead variations among the early members of the placental lineage. The oldest known metatherians are now not from eastern Asia but are 110 million years old from western North America, which produces a 50-million-year ghost lineage for Metatheria.

Over the past 20 years, more than 120 new genera of vertebrates have been described from the Early Cretaceous Jehol biota of northeastern China[1]. However, therian mammals—which include living placentals and marsupials as well as their respective broader clades, Eutheria and Metatheria—are rare at Jehol, and are represented by only three monotypic genera. Two of these genera, *Eomaia*[2] and *Acristatherium*[3], are widely accepted as eutherians[2–5], although the former was placed outside of Theria in a recent study[6] that was limited taxonomically by its inclusion of only three of the more than 40 known Cretaceous eutherians. The third Jehol therian, *Sinodelphys*[7], is generally considered to be the oldest known metatherian and to therefore provide morphological evidence for divergence of these two clades of living Theria. Here we describe a fourth Jehol therian and incorporate it into a phylogenetic analysis that supports all four Jehol therians as stem placentals.

Class Mammalia Linnaeus, 1758
Infraclass Eutheria sensu Huxley, 1880
Order incertae sedis
Family incertae sedis
Ambolestes gen. nov.
Ambolestes zhoui sp. nov.

Etymology. *Ambo* (Latin), both, in reference to the mixture of features previously held[7] to be from eutherians and metatherians; *lestes* (Greek), robber, a common ending for Cretaceous eutherians. The specific name *zhoui* is given in reference to Zhonghe Zhou, for his pioneering studies of the Jehol biota.

Holotype. A nearly complete skeleton preserved on main and counterpart slabs A and B of STM33-5 (Tianyu Museum of Nature, Linyi, Shandong Province, China) (Fig. 1, Extended Data Fig. 1 and Supplementary Tables 1, 2).

Locality and horizon. The holotype is from the Lower Cretaceous Yixian Formation at Xisanjia, Inner Mongolia, China, dated to about 126 million years ago (Ma)[8].

Diagnosis. Tooth formula: $I^{?}$:C^{1}:P^{5}:M^{3}/$I_{?}$:C_{1}:P_{4}:M_{3} (I, incisor; C, canine; P, premolar; M, molar; superscript and subscript denote upper and lower teeth, respectively) (Fig. 2 and Extended Data Figs. 2, 3). Differs from metatherians in that it has eight upper postcanine teeth, whereas metatherians have seven[9,10]. Differs from Jurassic and other Early Cretaceous eutherians known from full lower postcanine dentitions[2–5,11]—except for *Sinodelphys* (Extended Data Figs. 4, 5 and Supplementary Information) and *Sasayamamylos*[12]—in that it has seven lower postcanine teeth, whereas Jurassic and other Early Cretaceous eutherians have eight. Differs from *Sinodelphys*[7], *Sasayamamylos*[12] and *Montanalestes*[13] that possess a slightly medially inflected mandibular angle and metatherians[9,10] that possess a fully medially inflected angle: *Ambolestes* has a posteriorly directed mandibular angle as in *Eomaia*[2] and *Prokennalestes*[11]. Differs from *Sinodelphys*[7] in that it has a large trapezium in the wrist (Fig. 3a). Differs from *Sinodelphys*[7] and *Eomaia*[2] in that it has double-rooted upper canines. Differs from *Sinodelphys*[7], *Eomaia*[2] and *Acristatherium*[3] in that it has a first upper premolar that is smaller than the second. Differs from *Sinodelphys*[7], *Juramaia*[5] and *Eomaia*[2] in that it has a less-developed supraspinous fossa of the scapula and an enlarged parafibula. Differs from *Juramaia*[5], *Prokennalestes* and Late Cretaceous eutherians[4,11] in that it lacks a protocone or protoconal swelling on the ultimate upper premolar. Differs from *Sasayamamylos*[12] in that it has a lingual cingulid on the ultimate lower premolar, a Meckelian sulcus and masseteric foramen on the dentary (Extended Data Fig. 2). Differs from *Durlstotherium* and *Durlstodon* in that it has upper molars with a lower protocone and no conules[14]. Differs from the non-therians *Aegialodon*[15], *Kielantherium*, *Vincelestes*, *Peramus* and *Nanolestes*[4,11] in that it has a more-closed trigonid configuration on the lower molars.

Phylogenetic analyses

Phylogenetic analysis using parsimony (Supplementary Information) places the four Jehol therians (*Ambolestes*, *Sinodelphys*, *Acristatherium* and *Eomaia*) within Eutheria (Fig. 4 and Extended Data Fig. 6). The

---

[1]Yunnan Key Laboratory for Palaeobiology, Yunnan University, Kunming, China. [2]Department of Biology, Indiana University of Pennsylvania, Indiana, PA, USA. [3]Carnegie Museum of Natural History, Pittsburgh, PA, USA. [4]Institute of Geology and Paleontology, Linyi University, Linyi, China. [5]Tianyu Museum of Nature, Linyi, China. [6]Key Laboratory of Cenozoic Geology and Environment, Institute of Geology and Geophysics, Chinese Academy of Sciences, Beijing, China. [7]CAS Center for Excellence in Life and Paleoenvironment, Beijing, China. *e-mail: shundong.bi@iup.edu; wang_7355@163.com; wiblej@carnegiemnh.org

© 2018 Macmillan Publishers Limited, part of Springer Nature. All rights reserved.

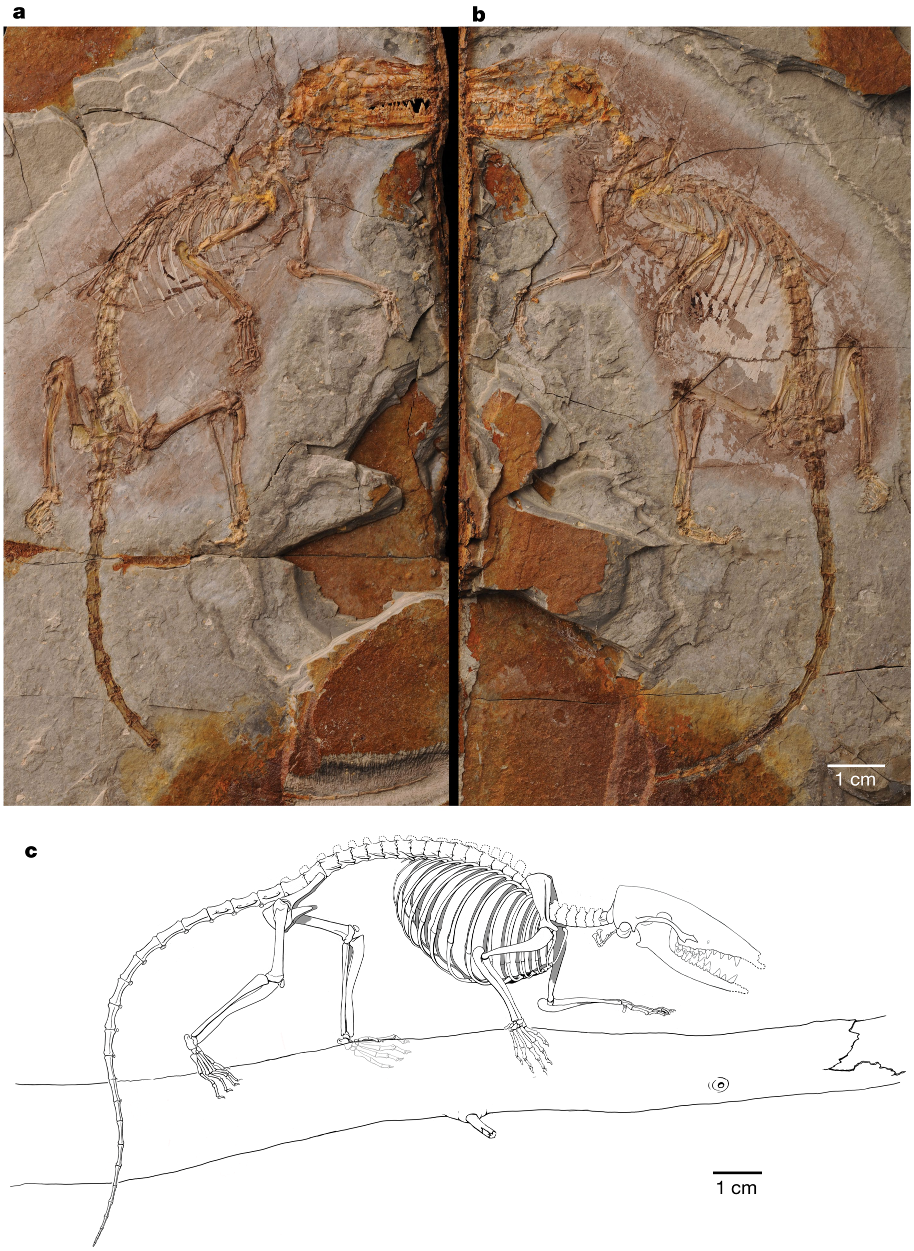

Fig. 1 | Holotype specimen of *A. zhoui* STM33-5, Tianyu Museum of Nature, Shandong Province, China. a, Main slab A. **b**, Counterpart slab B. **c**, Restoration.

first three are in a clade along with *Montanalestes* from the Early Cretaceous period of western North America[13], with *Ambolestes* in a sister relationship to *Sinodelphys*. The fourth Jehol therian, *Eomaia*, and the 160-million-year-old *Juramaia*—from the Tiaojishan Formation of northeastern China[5]—are sister to the clade that includes Placentalia. The major departure in our analyses that include *Ambolestes* from previous studies with a similar phylogenetic scope is the position of *Sinodelphys*, which had previously been identified at the base of Metatheria[5,7] and used to support an Asian origin for this clade[7]. Moreover, features of the wrist and ankle that distinguished *Sinodelphys* from the roughly contemporaneous *Eomaia* were used to support a fundamental dichotomy in the ways in which metatherians and eutherians attained their scansorial locomotory modes[7]. With *Sinodelphys* moved to Eutheria in our analysis, the oldest metatherians are represented by the sub-clades Deltatheroida and Marsupialiformes, which are both from the Albian (approximately 110 Ma) of western North America[16,17] (Fig. 4); the earliest members of these sub-clades from Asia are at least 20 million years younger[18,19]. Additionally, in the context of the new phylogenetic arrangement, the postcranial differences between *Sinodelphys* and *Eomaia* are not the result of metatherian–eutherian cladogenesis as had previously been suggested[7], but are instead variations within early eutherians. In the wrist example (Fig. 3a), *Sinodelphys* does share a large scaphoid, triquetrum, and hamate and small trapezium with many extant marsupials, and *Eomaia* shares the opposite state for these bones with some extant placentals. *Ambolestes* has a mixture of features of the two; it resembles *Sinodelphys* in possessing a large scaphoid, triquetrum and hamate, and *Eomaia* in possessing a large trapezium. The earliest members of Deltatheroida and Marsupialiformes are known only from isolated teeth and fragmentary jaws[16,17], and therefore provide no evidence of early metatherian locomotory adaptations.

Morphology of *Ambolestes*

In extant mammals, the ectotympanic bone is a component of the sound-conducting apparatus of the middle ear that provides an attachment for the tympanic membrane and the malleus—the latter either directly through bone (Fig. 5), or indirectly by ligament. Because of its delicate nature and because it is usually only loosely attached to

© 2018 Macmillan Publishers Limited, part of Springer Nature. All rights reserved.

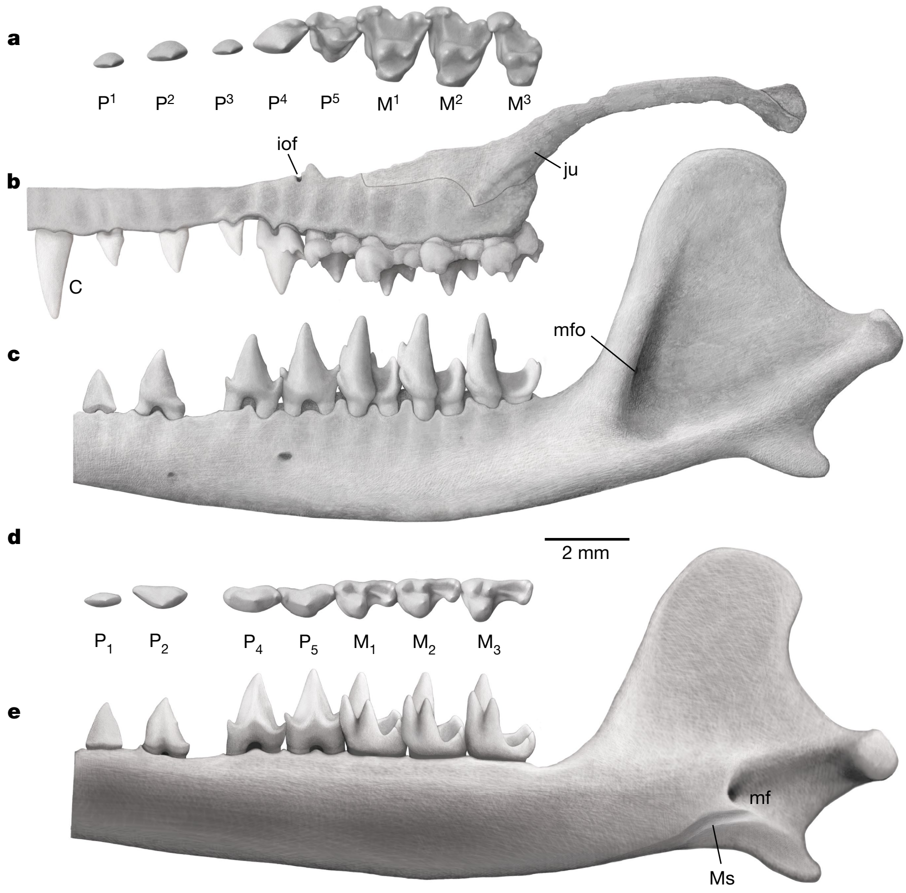

Fig. 2 | Dental and upper and lower jaw features of *A. zhoui* STM33-5. a, Left upper postcanine dentition in occlusal view. **b**, Left upper jaw in lateral view. **c**, Left dentary in lateral view. **d**, Left lower postcanine dentition in occlusal view. **e**, Right dentary in medial view. Lateral views in **b**, **c** are based on direct observation of the specimen; occlusal and lingual views in **a**, **d**, **e** are reconstructions based on direct observation of the specimen and on computed tomography scans. C, upper canine; iof, infraorbital foramen; ju, jugal; mf, mandibular foramen; mfo masseteric foramen; Ms, Meckel's sulcus. For the postcanine teeth: M, molar; P, premolar; and superscript and subscript numbers denote upper and lower teeth, respectively.

other bones, the ectotympanic is poorly known in Mesozoic mammaliaforms and our understanding of the evolution of this bone is therefore extremely limited. *Ambolestes* preserves both the left (Extended Data Fig. 2) and right ectotympanic bones. This C-shaped bone has a simple ring-shaped anterior crus (leg) and an expanded posterior crus (Fig. 5); the reverse condition occurs in the Late Cretaceous eutherians *Asioryctes*[20], *Uchkudukodon*[21] and *Zalambdalestes*[22], and in most extant therians. In the proportions of its crura, the ectotympanic of *Ambolestes* closely resembles that of some extant didelphid marsupials (opossums), especially *Monodelphis* (Fig. 5). As in opossums, the ectotympanic of *Ambolestes* has a distinct facet that curves around the rostral surface of the anterior crus (also seen in *Uchkudukodon*[21]), which held a similarly curved anterior process of the malleus (Fig. 5). In the C-shaped ectotympanic and curved anterior process of the malleus, *Ambolestes* and *Monodelphis* differ from non-therians such as the extant monotreme *Tachyglossus* and the eutriconodont *Liaoconodon*[23], in which the ectotympanic shape is not as uniformly curved and the anterior process of the malleus is straight (Fig. 5). These characteristics of the ectotympanic and malleus in *Tachyglossus* and *Liaoconodon* are retentions of the primitive arrangement of homologous structures in Mesozoic mammaliaforms such as *Morganucodon*, in which there was an osseous connection to the lower jaw through the postdentary bones[24]. This connection is retained in *Liaoconodon* through the ossified Meckel's cartilage[23] but is lost in *Tachyglossus*, as it is in all extant mammals. The short, shallow Meckelian sulcus in *Ambolestes* (Fig. 2) is a primitive retention that is lost in most therians, and its ectotympanic was probably fully suspended from the skull base as in extant mammals. The phylogenetic transformation of the shape of the ectotympanic and anterior process of the malleus from the straight non-therian to the curved therian pattern is traceable in the ontogeny of extant marsupials[25] (Fig. 5).

The hyoid apparatus in extant mammals sits in the floor of the mouth and provides attachment for muscles of the tongue, pharynx and body

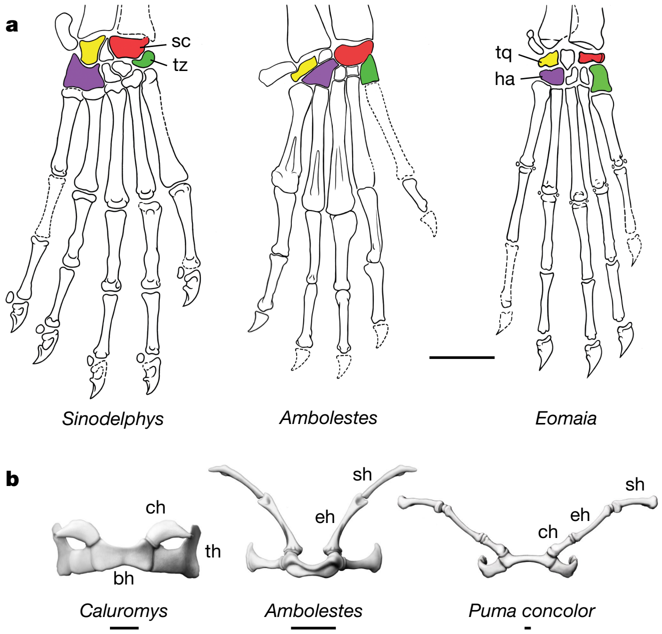

Fig. 3 | Forefoot and hyoid apparatus of *A. zhoui* compared with those of other mammals. a, Forefoot in dorsal view, of *Sinodelphys* (redrawn from a previous study[7]), *Ambolestes* STM33-5 and *Eomaia* (redrawn from a previous study[7]). **b**, Hyoid apparatus in ventral view in the extant didelphid marsupial *Caluromys derbianus* (Carnegie Museum of Natural History CM 119051), *Ambolestes* STM33-5 and the extant carnivoran *Puma concolor* (Carnegie Museum of Natural History CM 59940). bh, basihyal; ch, ceratohyal; eh, epihyal; ha, hamate; sc, scaphoid; sh, stylohyal; th, thyrohyal; tq, triquetrum; tz, trapezium. Scale bars, 2 mm.

© 2018 Macmillan Publishers Limited, part of Springer Nature. All rights reserved.

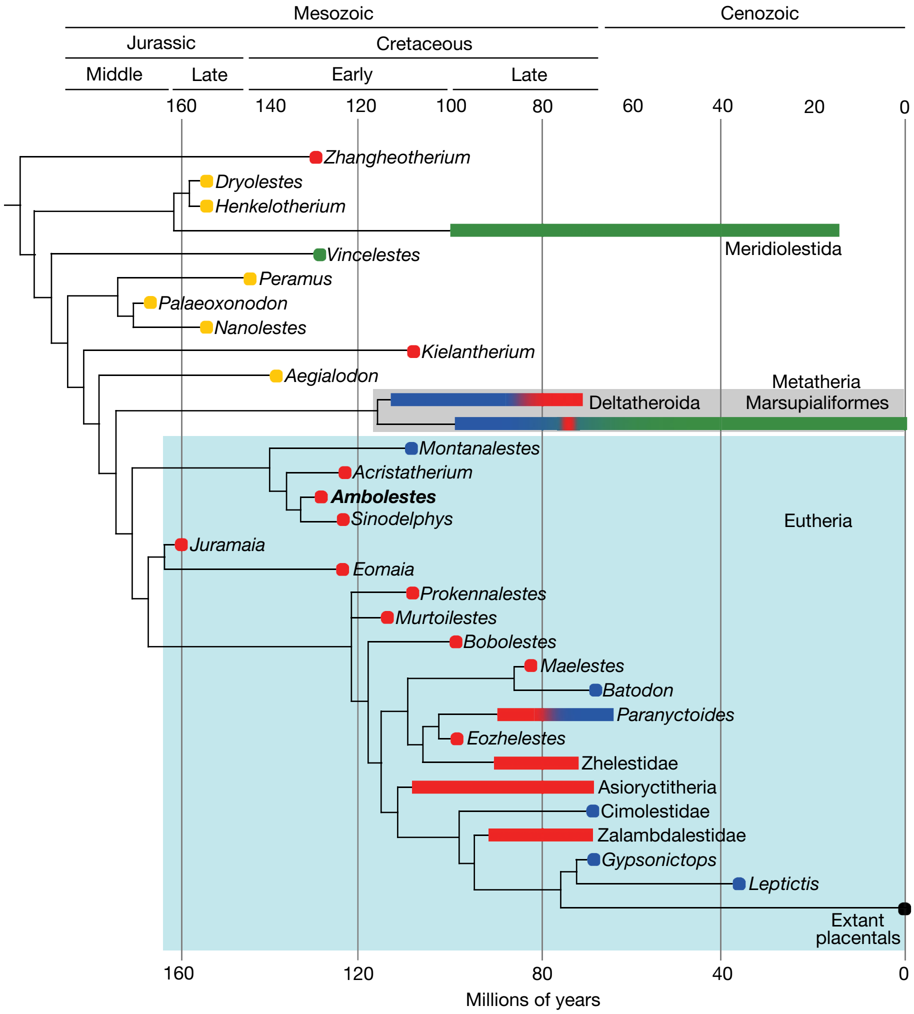

Fig. 4 | Relationships of *A. zhoui* to other mammals. Simplified tree of the strict consensus of the four most-parsimonious trees (Supplementary Information). Colours indicate current continent of discovery for the specimens studied here (except Placentalia): red, Asia; yellow, Europe; green, South America; blue, North America. Deltatheroida, Marsupialiformes and *Paranyctoides* are mixed, with specimens found on different continents.

wall[26]. Three bones (the unpaired basihyal and paired thyrohyals) form a basal series possessed by all mammals. Four paired bones—the ceratohyals, epihyals, stylohyals and tympanohyals (for example, *Puma* in Fig. 3b)—are variably present and may form a suspensory series; tympanohyals are usually fused to the petrosal bone on the skull base. In situations in which one or more parts of the suspensory series fail to ossify (for example, *Caluromys* in Fig. 3b), the stylohyoid ligament connects the basal series to the basicranium. The number of individual bones varies from nine (for example, *Puma* in Fig. 3b) to as few as one (as in humans, albeit one formed from six ossification centres[27]). The number and shape of the elements has some phylogenetic value as, for example, all marsupials have the same five elements[26] (see *Caluromys* in Fig. 3b). The evolution of the mammalian hyoid is poorly known because few of these bones are preserved in the fossil record. Possible hyoid fragments have been noted for some Mesozoic mammals (including *Maotherium*[28], *Liaoconodon*[23] and *Vilevolodon*[29]) but a complete series has not previously been reported. The hyoid apparatus in *Ambolestes* is complete and composed of seven elements (Fig. 3b). Of the extant mammals studied to date, the only ones to possess the same elements as those present in *Ambolestes* are in the squirrel family, including all tree squirrels and some terrestrial squirrels[30]. In the squirrels, the unpaired basihyal and paired thyrohyals, epihyals and stylohyals[30] are present, and we identify the elements in *Ambolestes* accordingly. As with other parts of the anatomy, the hyoid of *Ambolestes* has a mosaic of marsupial and placental features. The basal series of *Ambolestes* resembles that of marsupials in terms of its basihyal, which is much shorter than the thyrohyals, but differs from marsupials and resembles many placentals in having a continuous ossified suspensory series (Fig. 3b).

With an estimated body weight of 34–44 g (Supplementary Information)—roughly equivalent to an extant mouse opossum (*Marmosa*)—*Ambolestes* is similar in size to other Jehol eutherians[2,3,7], whereas the Jurassic *Juramaia* is smaller at 15–17 g[5]. *Eomaia* and *Sinodelphys*, both of which are known from postcranial bones, were originally suggested to be scansorial, primarily on the basis of their manual and pedal digit proportions[2,7]. A recent and more comprehensive study of these elements identified *Eomaia* as arboreal and *Sinodelphys* as scansorial[31]. The manual digit proportions and intermembral index of *Ambolestes* resemble those of *Eomaia* more than those of *Sinodelphys* (Extended Data Fig. 7); therefore, depending on which authors are followed, *Ambolestes* may be regarded as either scansorial or arboreal—categories that do not in any case separate cleanly with most metrics[31]. Regardless of what may have been happening elsewhere, the taxa from the Jehol biota demonstrate that arboreality was an important theme in the diversification of early Eutheria.

Eutherian–metatherian divergence

Merging recent molecular estimates for the divergence of Eutheria and Metatheria[32,33] results in a broad temporal range for this event, from the earliest Cretaceous to the latest Triassic period (140–215 Ma). Only three therian fossils, each purported to be a eutherian[5,14], have been found within this range and therefore have the potential to provide some support for the molecular estimates.

© 2018 Macmillan Publishers Limited, part of Springer Nature. All rights reserved.

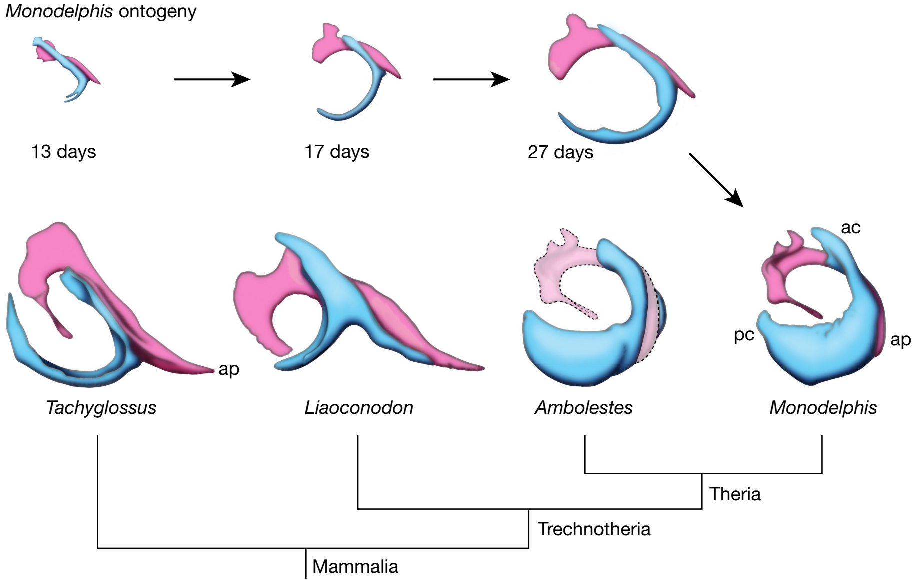

Fig. 5 | Ectotympanic and malleus in *A. zhoui* and other mammals. Bottom row shows ectotympanic (blue) and malleus (pink) of the extant monotreme *Tachyglossus aculeatus* (Carnegie Museum of Natural History CM 50809), the Jehol eutriconodont *Liaoconodon hui* (redrawn from a previous study[23]), *Ambolestes*, and the extant didelphid *Monodelphis domestica*, (Carnegie Museum of Natural History CM 80017). Not to scale. Top row shows *M. domestica* at postnatal days 13, 17 and 27 (from a previously published computed tomography dataset[25]). Shown to scale with adult *Monodelphis* in bottom row. The malleus is not known for *Ambolestes*: the anterior process is reconstructed based on the facet on the anterior crus of the ectotympanic. ac, anterior crus of ectotympanic; ap, anterior process of malleus; pc, posterior crus of ectotympanic.

These are 160-million-year-old *Juramaia*, represented by a relatively complete dentition[5] (Extended Data Fig. 4), and the 145-million-year-old *Durlstotherium* and *Durlstodon* from southern England, each of which is represented by only an incomplete upper ultimate molar[14]. Despite the 35 million years that separate *Juramaia* from the Jehol eutherian *Eomaia*, their dentitions share numerous similarities that form the primary basis for their sister-group relationship in our analysis (Fig. 4). *Durlstotherium* and *Durlstodon* exhibit a similar phenomenon; their upper ultimate molars are unexpectedly advanced and resemble those of younger taxa. However, for *Durlstotherium* and *Durlstodon* this separation is more in the range of 50 million years, as the younger taxa are early Late Cretaceous eutherians with upper ultimate molars that have conules and high protocones[4,11]. How can these unexpected resemblances across vast geological time be explained? For *Juramaia*, the stratigraphic position of the only known specimen has been questioned[34], with a suggested younger age that appears to have been based on the notable similarities to geologically younger taxa. An alternative explanation for these unexpected resemblances is the early appearance of a derived morphology coupled to a slow rate of dental change. However, with so few data points across this initial phase of eutherian evolutionary history an informed conclusion is not possible. If the molecular estimates are appropriate, mammalian palaeontologists face the challenge of finding more fossils that are contemporaneous with the molecular estimates for the eutherian side—and finding any fossils for the metatherian side, for which a 50-million-year ghost lineage now exists.

Online content

Any Methods, including any statements of data availability and Nature Research reporting summaries, along with any additional references and Source Data files, are available in the online version of the paper at https://doi.org/10.1038/s41586-018-0210-3.

Received: 27 April 2018; Accepted: 10 May 2018;
Published online: 13 June 2018

1. Zhou, Z. & Wang, Y. Vertebrate diversity of the Jehol Biota as compared with other lagerstätten. *Sci. China Earth Sci.* **53**, 1894–1907 (2010).
2. Ji, Q. et al. The earliest known eutherian mammal. *Nature* **416**, 816–822 (2002).
3. Hu, Y., Meng, J., Li, C. & Wang, Y. New basal eutherian mammal from the Early Cretaceous Jehol biota, Liaoning, China. *Proc. R. Soc. Lond. B* **277**, 229–236 (2010).
4. Wible, J. R., Rougier, G. W., Novacek, M. J. & Asher, R. J. The eutherian mammal *Maelestes gobiensis* from the Late Cretaceous of Mongolia and the phylogeny of Cretaceous Eutheria. *Bull. Am. Mus. Nat. Hist.* **327**, 1–123 (2009).
5. Luo, Z.-X., Yuan, C.-X., Meng, Q.-J. & Ji, Q. A Jurassic eutherian mammal and divergence of marsupials and placentals. *Nature* **476**, 442–445 (2011).
6. O'Leary, M. A. et al. The placental mammal ancestor and the post-K-Pg radiation of placentals. *Science* **339**, 662–667 (2013).
7. Luo, Z.-X., Ji, Q., Wible, J. R. & Yuan, C.-X. An Early Cretaceous tribosphenic mammal and metatherian evolution. *Science* **302**, 1934–1940 (2003).
8. Chang, S.-C., Gao, K.-Q., Zhou, C.-F. & Jourdan, F. New chronostratigraphic constraints on the Yixian Formation with implications for the Jehol Biota. *Palaeogeogr. Palaeoclimatol. Palaeoecol.* **487**, 399–406 (2017).
9. Williamson, T. E., Brusatte, S. L. & Wilson, G. P. The origin and early evolution of metatherian mammals: the Cretaceous record. *ZooKeys* **465**, 1–76 (2014).
10. Bi, S., Jin, X., Li, S. & Du, T. A new Cretaceous metatherian mammal from Henan, China. *PeerJ* **3**, e896 (2015).
11. Averianov, A. O. & Archibald, D. in *Legacy of the Gobi Desert: Papers in Memory of Zofia Kielan-Jaworowska (Palaeontologia Polonica 67)* (eds Cifelli, R. L. & Fostowicz-Frelik, Ł.) 25–33 (Institute of Paleobiology of the Polish Academy of Sciences, Warsaw, 2016).
12. Kusuhashi, N. et al. A new Early Cretaceous eutherian mammal from the Sasayama Group, Hyogo, Japan. *Proc. R. Soc. Lond. B* **280**, 20130142 (2013).
13. Cifelli, R. L. Tribosphenic mammal from the North American Early Cretaceous. *Nature* **401**, 363–366 (1999).
14. Sweetman, S. C., Smith, G. & Martill, D. M. Highly derived eutherian mammals from the earliest Cretaceous of southern Britain. *Acta Palaeontol. Pol.* **62**, 657–665 (2017).
15. Kermack, K. A., Lees, P. M. & Mussett, F. *Aegialodon dawsoni*, a new trituberculosectorial tooth from the Lower Wealden. *Proc. R. Soc. Lond. B* **162**, 535–554 (1965).
16. Davis, B. M., Cifelli, R. L. & Kielan-Jaworowska, Z. in *Mammalian Evolutionary Morphology: a Tribute to Frederick S. Szalay* (eds Sargis, E. J. & Dagosto, M.) 3–24 (Springer, Dordrecht, 2008).
17. Cifelli, R. L. & Davis, B. M. Tribosphenic mammals from the Lower Cretaceous Cloverly Formation of Montana and Wyoming. *J. Vertebr. Paleontol.* **35**, e920848 (2015).
18. Averianov, A. O., Archibald, J. D. & Ekdale, E. G. New material of the Late Cretaceous deltatheroidan mammal *Sulestes* from Uzbekistan and phylogenetic reassessment of the metatherian–eutherian dichotomy. *J. Syst. Palaeontol.* **8**, 301–330 (2010).
19. Szalay, F. S. & Trofimov, B. A. The Mongolian Late Cretaceous *Asiatherium*, and the early phylogeny and paleobiogeography of Metatheria. *J. Vertebr. Paleontol.* **16**, 474–509 (1996).
20. Kielan-Jaworowska, Z. in *Results of the Polish–Mongolian Palaeontological Expeditions. Part IX. (Palaeontologia Polonica 42)* (ed. Kielan-Jaworowska, Z.) 25–78 (Institute of Paleobiology of the Polish Academy of Sciences, Warsaw, 1981).

© 2018 Macmillan Publishers Limited, part of Springer Nature. All rights reserved.

21. McKenna, M. C., Kielan-Jaworowska, Z. & Meng, J. Earliest eutherian mammal skull from the Late Cretaceous (Coniacian) of Uzbekistan. *Acta Palaeontol. Pol.* **45**, 1–54 (2000).
22. Wible, J. R., Novacek, M. J. & Rougier, G. W. New data on the skull and dentition in the Mongolian Late Cretaceous eutherian mammal *Zalambdalestes*. *Bull. Am. Mus. Nat. Hist.* **281**, 1–144 (2004).
23. Meng, J., Wang, Y. & Li, C. Transitional mammalian middle ear from a new Cretaceous Jehol eutriconodont. *Nature* **472**, 181–185 (2011).
24. Luo, Z.-X. Developmental patterns in Mesozoic evolution of mammal ears. *Annu. Rev. Ecol. Evol. Syst.* **42**, 355–380 (2011).
25. Ramírez-Chaves, H. E. et al. Mammalian development does not recapitulate suspected key transformations in the evolutionary detachment of the mammalian middle ear. *Proc. R. Soc. Lond. B* **283**, 20152606 (2016).
26. Gasc, J.-P. in *Traité de Zoologie tome* XVI, fasc. 1 (ed. Grassé, P.-P.) 550–583, 1103–1106 (Masson, Paris, 1971).
27. Standring, S. (ed.) *Gray's Anatomy: the Anatomical Basis of Clinical Practice* 40th edn (Churchill Livingstone, Edinburgh, 2008).
28. Rougier, G. W., Ji, Q. & Novacek, M. J. A new symmetrodont mammal with fur impressions from the Mesozoic of China. *Acta Geol. Sin.* **77**, 7–14 (2003).
29. Luo, Z.-X. et al. New evidence for mammaliaform ear evolution and feeding adaptation in a Jurassic ecosystem. *Nature* **548**, 326–329 (2017).
30. Hoffmeister, R. G. & Hoffmeister, D. F. The hyoid in North American squirrels, Sciuridae, with remarks on associated musculature. *An. Inst. Biol. Univ. Nac. Auton. Mex. Ser. Zool.* **62**, 219–234 (1991).
31. Chen, M. & Wilson, G. P. A multivariate approach to infer locomotor modes in Mesozoic mammals. *Paleobiology* **41**, 280–312 (2015).
32. Meredith, R. W. et al. Impacts of the Cretaceous terrestrial revolution and KPg extinction on mammal diversification. *Science* **334**, 521–524 (2011).
33. dos Reis, M. et al. Phylogenomic datasets provide both precision and accuracy in estimating the timescale of placental mammal phylogeny. *Proc. R. Soc. Lond. B* **279**, 3491–3500 (2012).
34. Meng, J. Mesozoic mammals of China: implications for phylogeny and early evolution of mammals. *Natl Sci. Rev.* **1**, 521–542 (2014).

Acknowledgements We thank S. Xie for specimen preparation; P. Bowden for illustration; W. Gao for photography; Y. Hou and P. Yin for computed tomography scanning; D. Koyabu and V. Weisbecker for providing the computed tomography dataset of *Monodelphis*; and J. Meng, X. Xu, B. Jiang and Y. Huang for assistance and discussion. The study was supported by the National Natural Science Foundation of China (41688103, 41728003, 41372014, 41472023) and Chinese Academy of Sciences (XDPB0503). Support for S.B. was provided by the MEC International Joint Laboratory for Palaeobiology and Palaeoenvironment, Yunnan University. Support for J.R.W. is provided by the National Science Foundation Grant DEB 1654949 and Carnegie Museum of Natural History.

Reviewer information *Nature* thanks R. Cifelli, D. Krause and G. Rougier for their contribution to the peer review of this work.

Author contributions S.B. and J.R.W. conceived the study, undertook comparative and analytical work and wrote the paper; N.E.C. performed the ternary plot; and X.Z., S.Y. and X.W. contributed to fossil interpretation and provided feedback to the paper.

Competing interests The authors declare no competing interests.

Additional information

Extended data is available for this paper at https://doi.org/10.1038/s41586-018-0210-3.
Supplementary information is available for this paper at https://doi.org/10.1038/s41586-018-0210-3.
Reprints and permissions information is available at http://www.nature.com/reprints.
Correspondence and requests for materials should be addressed to S.B. or X.W. or J.R.W.
Publisher's note: Springer Nature remains neutral with regard to jurisdictional claims in published maps and institutional affiliations.

© 2018 Macmillan Publishers Limited, part of Springer Nature. All rights reserved.

METHODS

Computed tomography scanning. The skull of the main slab (A) of *Ambolestes* STM33-5 (Fig. 1a and Extended Data Fig. 1a) was scanned with the 225-kV micro-CT at the Key Laboratory of Vertebrate Evolution and Human Origin of CAS. A total of 1,797 transmission images were reconstructed in a 518 × 518 matrix of 727 slices in two-dimensional reconstruction software developed by the Institute of High Energy Physics, CAS. The three-dimensional reconstructions were created with the software Mimics (version 16.1).

Phylogenetic analysis. The data matrix consisting of 64 taxa and 401 characters was analysed in TNT[35] under the new technology search (sectorial search, ratchet, tree fusing) set to 100 iterations, followed by a traditional search. All characters were equally weighted and non-additive. The search procedure resulted in four most-parsimonious trees (MPTs) of length 1,776 (consistency index = 0.319; retention index = 0.598). The strict consensus tree (1,779 steps; consistency index = 0.318; retention index = 0.597) of these four MPTs is presented in Fig. 4. The list of the synapomorphies common to the four MPTs was produced using the 'Common Synapomorphies' options in TNT. A list of synapomorphies for the clades Eutheria, Metatheria and the clade formed by *Ambolestes* and *Sinodelphys* is provided in the Supplementary Information.

Reporting summary. Further information on experimental design is available in the Nature Research Reporting Summary linked to this paper.

Data availability. The new specimens analysed in this study have been deposited at the Tianyu Museum of Nature, Linyi, Shandong Province, China. Graphics and phylogenetics data are provided in the Supplementary Information. Life Science Identifiers (LSID) for the new genus and species are registered with Zoobank (http://zoobank.org): urn:lsid:zoobank.org:act:6DC5CD12-44DE-4C5E-B90C-EDA0481695E3 and urn:lsid:zoobank.org:act:4A18FEDF-039B-46F7-836F-A6B147E50DCC. The data matrix for the phylogenetic analysis has been deposited in MorphoBank (http://morphobank.org/permalink/?P2799).

35. Goloboff, P. A., Farris, J. S. & Nixon, K. C. TNT, a free program for phylogenetic analysis. *Cladistics* **24**, 774–786 (2008).

© 2018 Macmillan Publishers Limited, part of Springer Nature. All rights reserved.

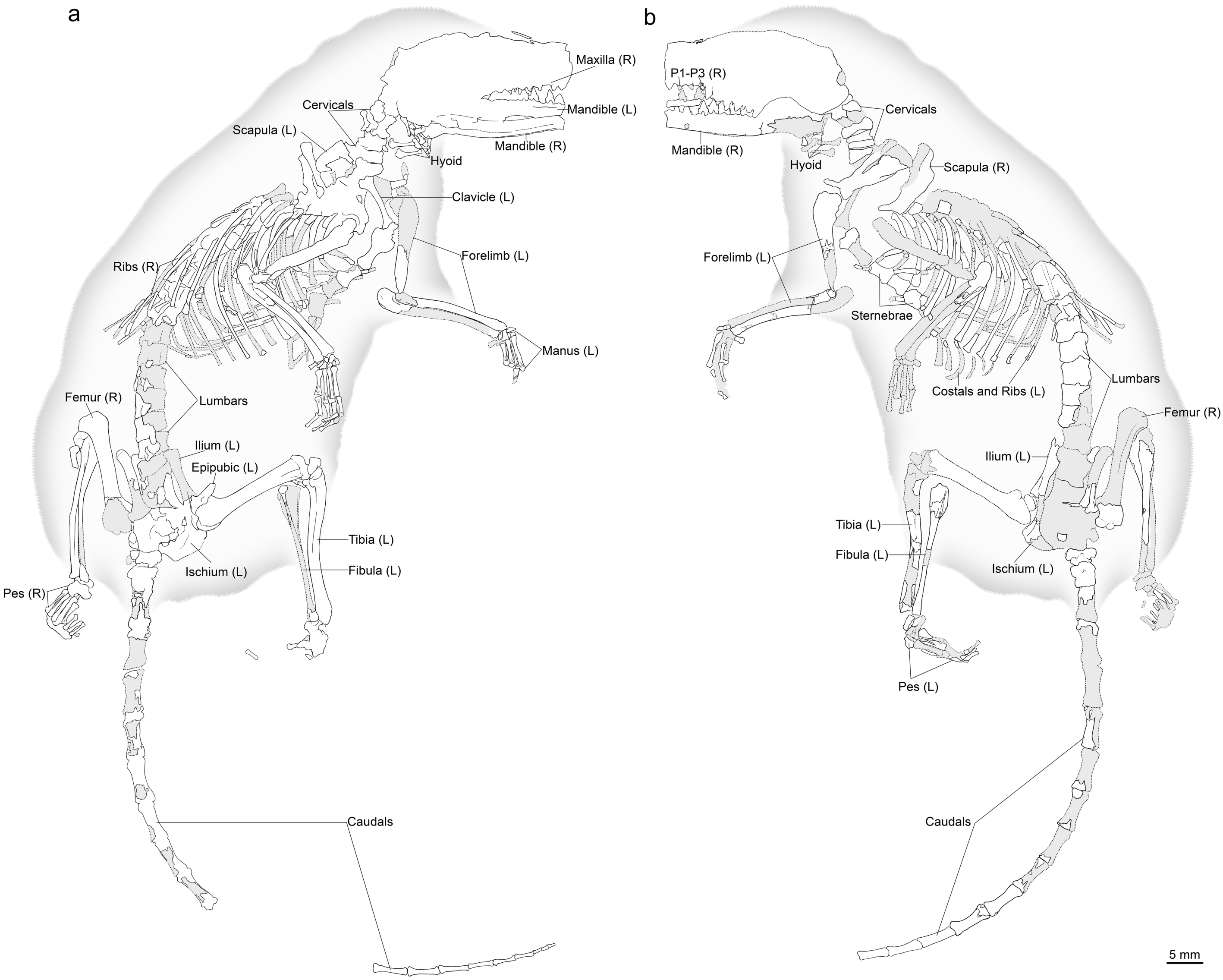

Extended Data Fig. 1 | Line drawings of *A. zhoui* STM33-5. a, Main slab. **b**, Counterpart slab.

© 2018 Macmillan Publishers Limited, part of Springer Nature. All rights reserved.

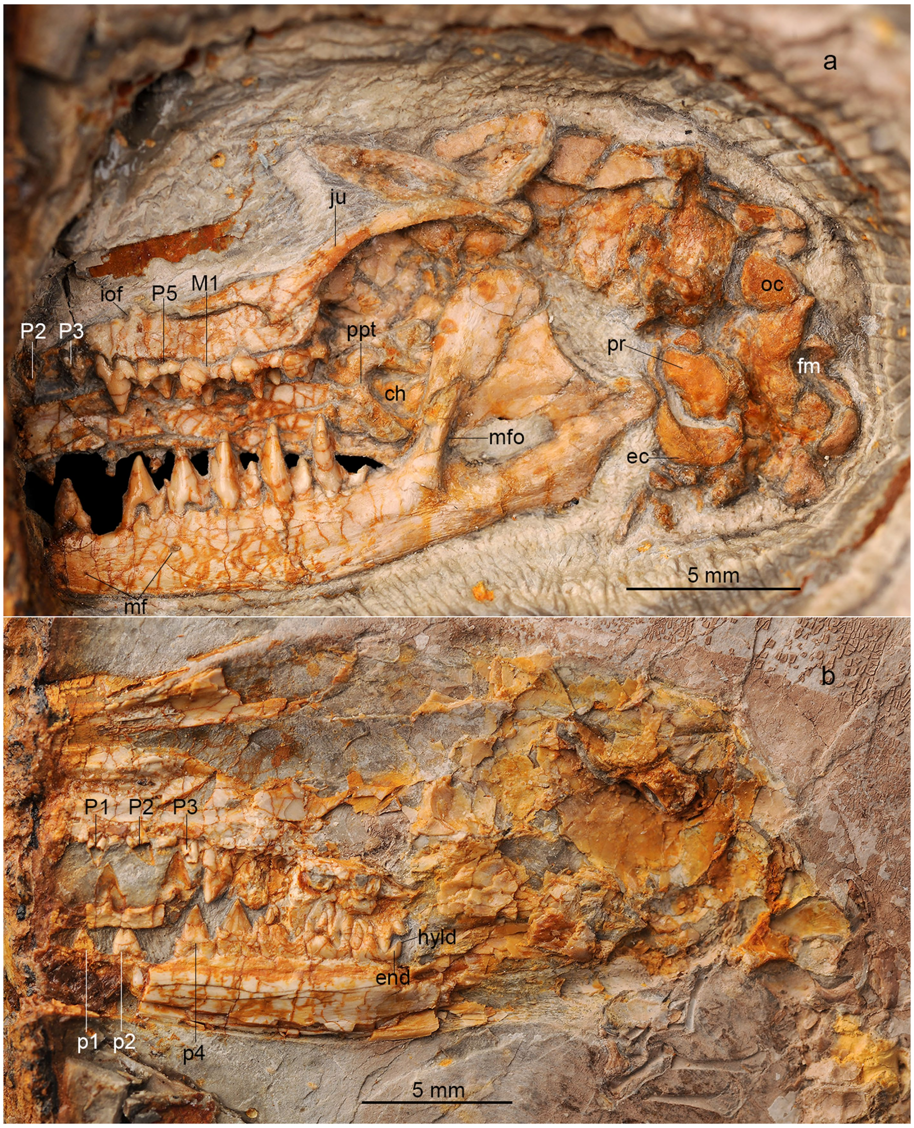

Extended Data Fig. 2 | Close-up views of craniodental features of *A. zhoui* STM33-5. a, Partial skull and left dentary of the main slab in lateral view. **b**, Partial skull and right dentary of the counterpart slab in medial view. M and m, upper and lower molars, respectively; P and p, upper and lower premolars, respectively. ch, choanae; ec, ectotympanic; end, entoconid; fm, foramen magnum; hyld, hypoconulid; iof, infraorbital foramen; ju, jugal; mf, mental foramina; mfo, masseteric foramen; oc, occipital condyle; ppt, postpalatine torus; pr, promontorium of petrosal.

© 2018 Macmillan Publishers Limited, part of Springer Nature. All rights reserved.

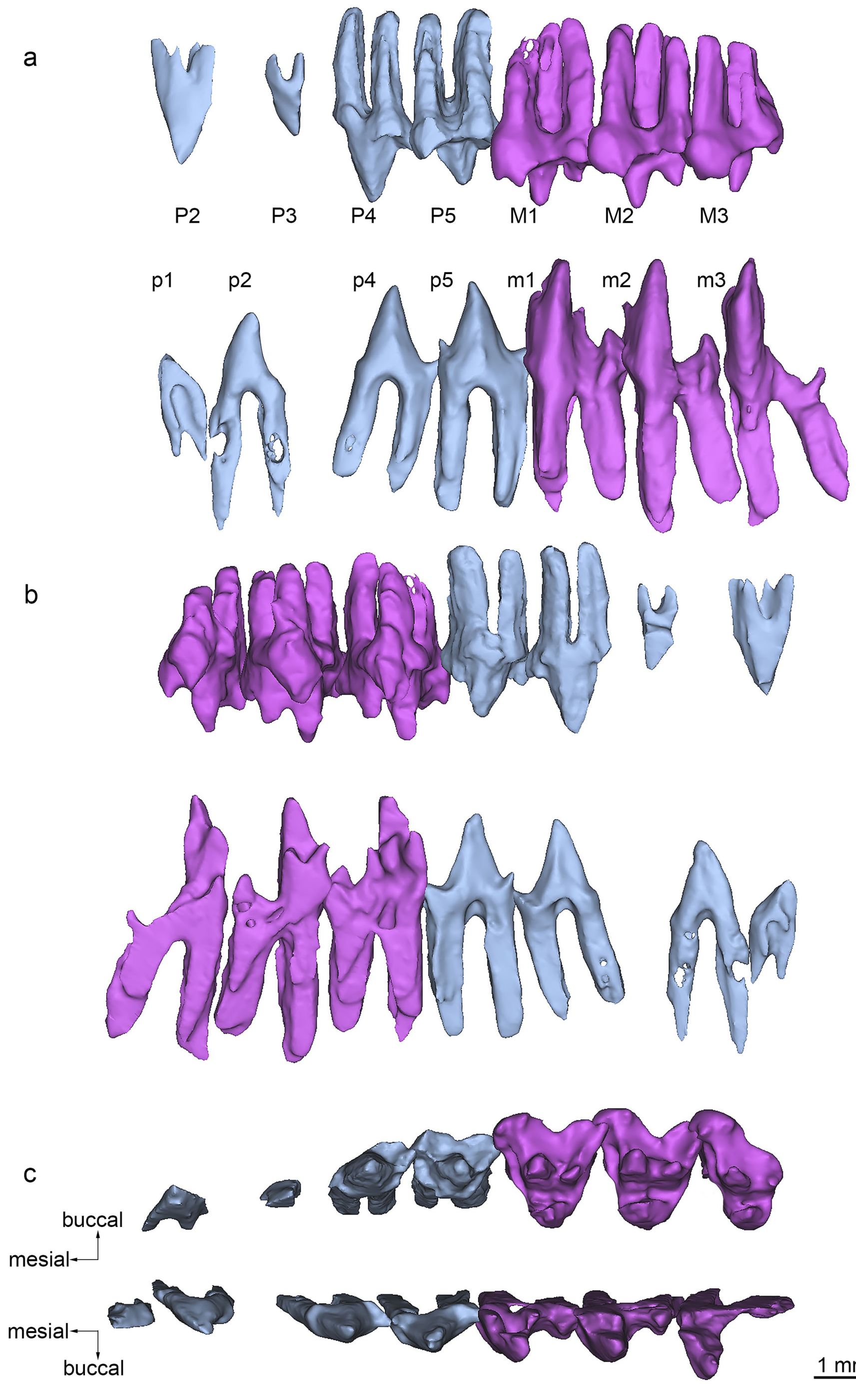

Extended Data Fig. 3 | Left upper and lower teeth of *A. zhoui* STM33-5 as preserved on the main slab (A) of the specimen from 3D rendering (Mimics) of computed tomography scans. a, Buccal view. **b**, Lingual view. **c**, Occlusal view. The lingual face of M_1–M_3, including the entoconid and hypoconulid, has been sheared off.

© 2018 Macmillan Publishers Limited, part of Springer Nature. All rights reserved.

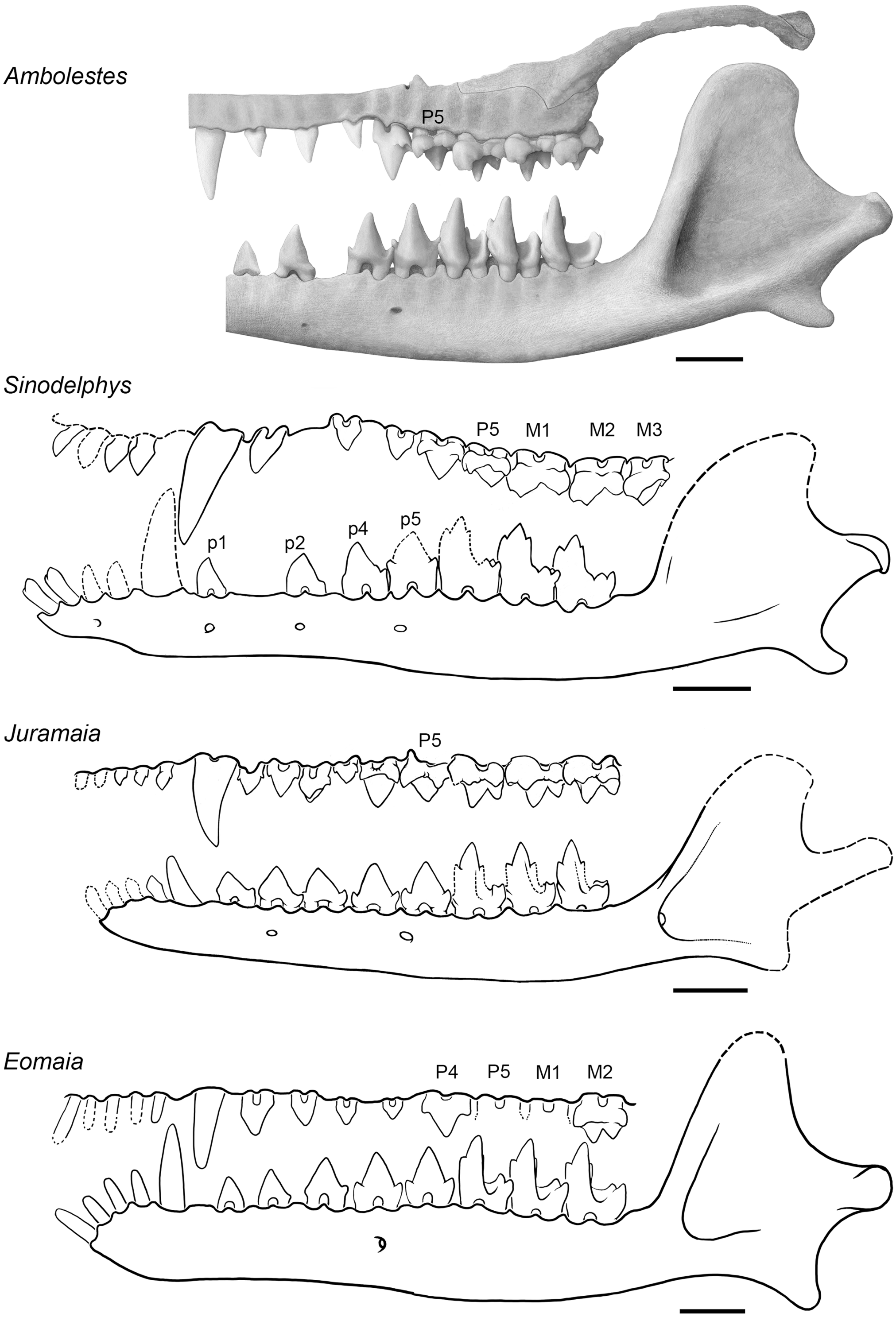

Extended Data Fig. 4 | Comparison of left upper and lower jaws in lateral view of *Ambolestes*, *Sinodelphys*, *Juramaia* and *Eomaia*. *Sinodelphys* was redrawn from a previous study[7] and reversed from the original; *Juramaia* was redrawn from a previous study[5]; and *Eomaia* was redrawn from a previous study[2] and reversed from the original. Scale bars, 2 mm.

© 2018 Macmillan Publishers Limited, part of Springer Nature. All rights reserved.

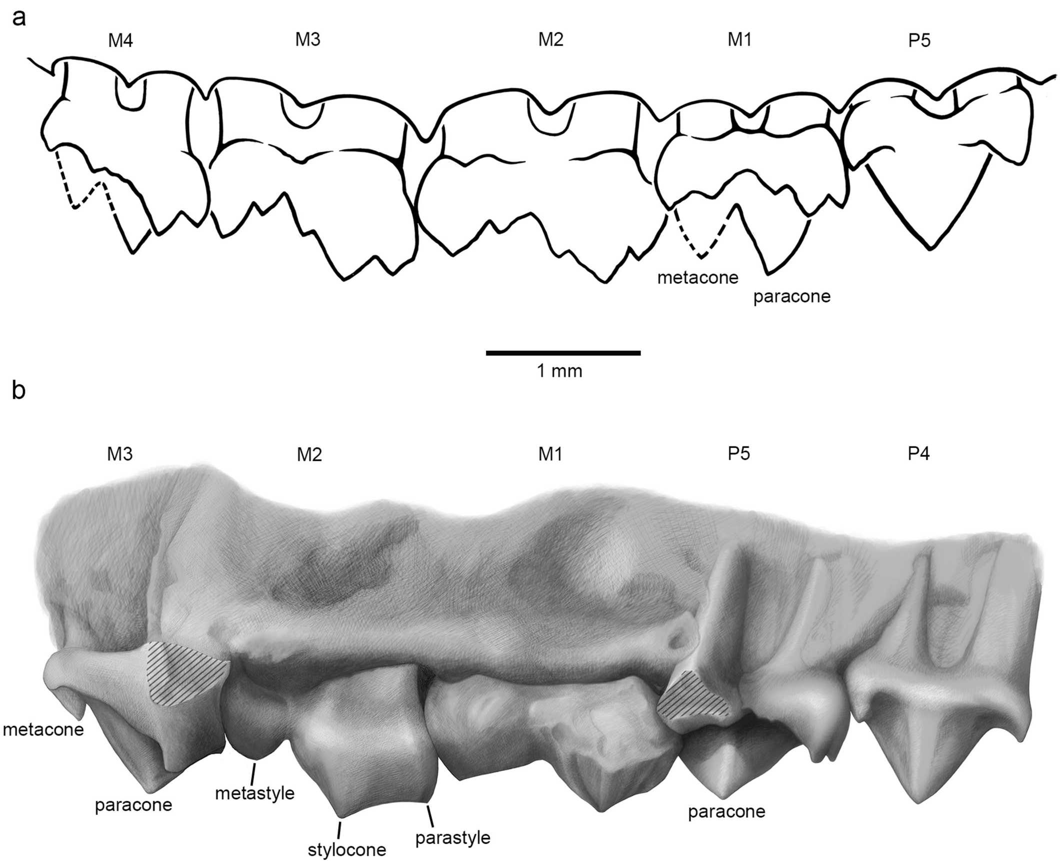

Extended Data Fig. 5 | Left upper dentition of *Sinodelphys szalayi*. **a**, Dental formula redrawn from a previous study[7]. **b**, Dental formula proposed in this work on drawing of CM 79002 (a cast of the holotype). Note that the tooth identified as M^1 in the previous study[7] is not molariform, but is instead built on the same pattern as the tall, trenchant premolariform tooth that is mesial to it. On the M^1 and M^2 (as interpreted here), the paracone and metacone are hidden by the stylar shelf.

© 2018 Macmillan Publishers Limited, part of Springer Nature. All rights reserved.

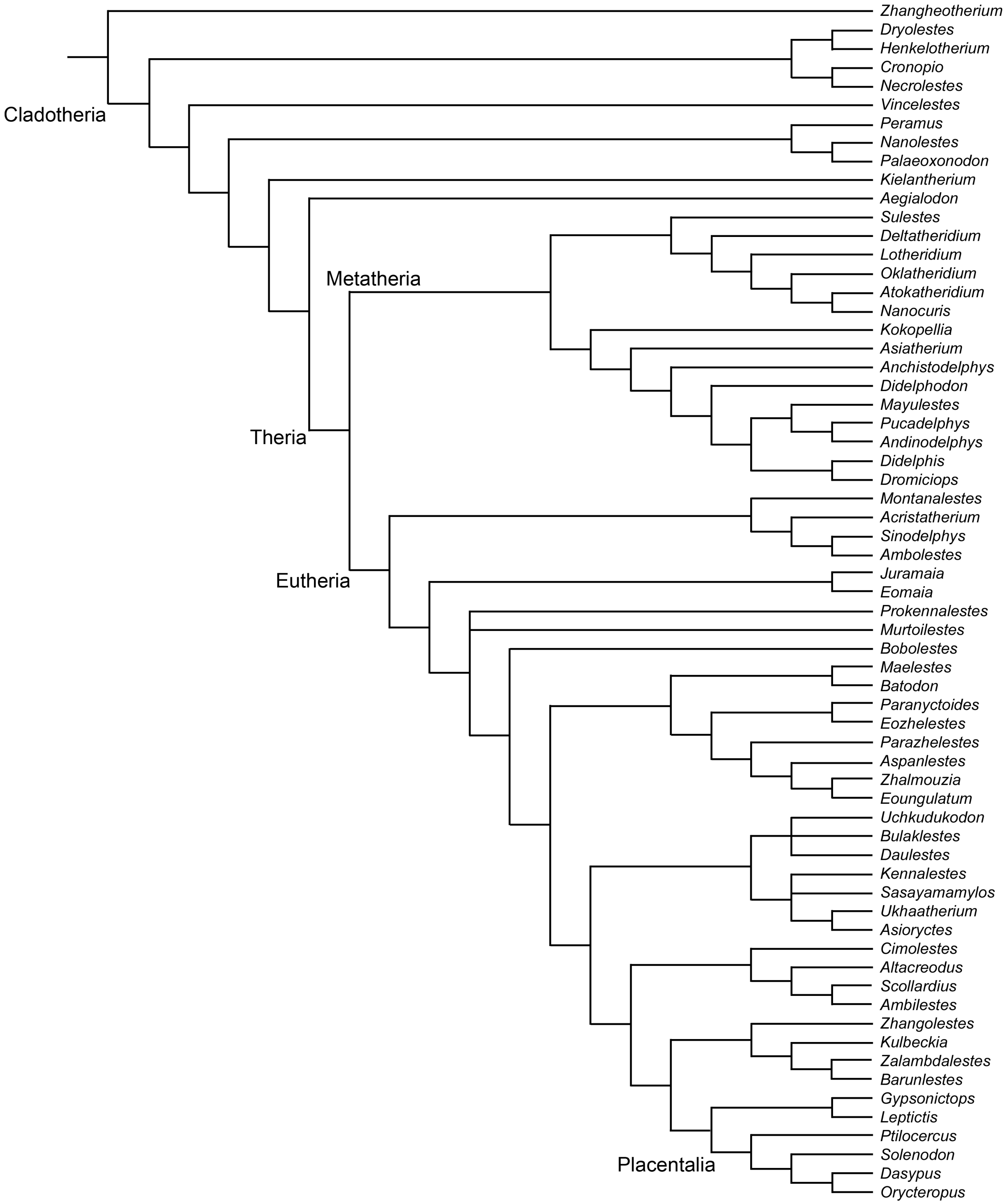

Extended Data Fig. 6 | The strict consensus tree of four equally most-parsimonious trees. The consensus tree length = 1,779, consistency index = 0.318 and retention index = 0.597. A simplified version of this consensus tree is presented in Fig. 4.

© 2018 Macmillan Publishers Limited, part of Springer Nature. All rights reserved.

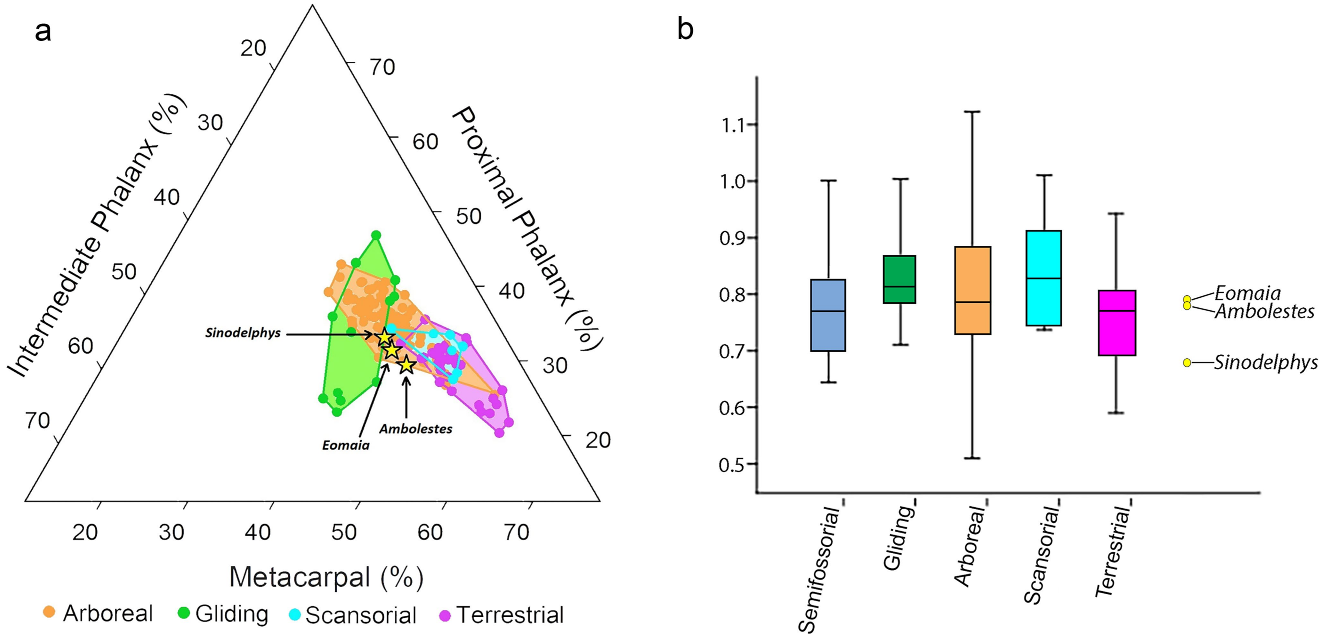

Extended Data Fig. 7 | Analysis of limb elements of *A. zhoui* STM33-5 for locomotor behaviour. a, Ternary plot showing intrinsic manual ray III proportions. **b**, Box plots of the intermembral index. The line that divides the box into two parts represents the median, the box shows the upper and lower quartiles, and the whiskers show extreme values for each group.

© 2018 Macmillan Publishers Limited, part of Springer Nature. All rights reserved.

nature research

Corresponding author(s): Shundong Bi and John R. Wible

Reporting Summary

Nature Research wishes to improve the reproducibility of the work that we publish. This form provides structure for consistency and transparency in reporting. For further information on Nature Research policies, see Authors & Referees and the Editorial Policy Checklist.

Statistical parameters

When statistical analyses are reported, confirm that the following items are present in the relevant location (e.g. figure legend, table legend, main text, or Methods section).

n/a	Confirmed	
☐	☒	The exact sample size (n) for each experimental group/condition, given as a discrete number and unit of measurement
☒	☐	An indication of whether measurements were taken from distinct samples or whether the same sample was measured repeatedly
☒	☐	The statistical test(s) used AND whether they are one- or two-sided *Only common tests should be described solely by name; describe more complex techniques in the Methods section.*
☒	☐	A description of all covariates tested
☒	☐	A description of any assumptions or corrections, such as tests of normality and adjustment for multiple comparisons
☒	☐	A full description of the statistics including central tendency (e.g. means) or other basic estimates (e.g. regression coefficient) AND variation (e.g. standard deviation) or associated estimates of uncertainty (e.g. confidence intervals)
☒	☐	For null hypothesis testing, the test statistic (e.g. F, t, r) with confidence intervals, effect sizes, degrees of freedom and P value noted *Give P values as exact values whenever suitable.*
☒	☐	For Bayesian analysis, information on the choice of priors and Markov chain Monte Carlo settings
☒	☐	For hierarchical and complex designs, identification of the appropriate level for tests and full reporting of outcomes
☒	☐	Estimates of effect sizes (e.g. Cohen's d, Pearson's r), indicating how they were calculated
☒	☐	Clearly defined error bars *State explicitly what error bars represent (e.g. SD, SE, CI)*

Our web collection on statistics for biologists may be useful.

Software and code

Policy information about availability of computer code

Data collection	No software was used.
Data analysis	TNT version 1.5 was used for phylogenetic analyses and Mimics version 16.1 was used for 3D reconstructions.

For manuscripts utilizing custom algorithms or software that are central to the research but not yet described in published literature, software must be made available to editors/reviewers upon request. We strongly encourage code deposition in a community repository (e.g. GitHub). See the Nature Research guidelines for submitting code & software for further information.

Data

Policy information about availability of data

All manuscripts must include a data availability statement. This statement should provide the following information, where applicable:

- Accession codes, unique identifiers, or web links for publicly available datasets
- A list of figures that have associated raw data
- A description of any restrictions on data availability

All specimens of this study have been deposited at the Tianyu Museum of Nature. The data matrix for the phylogenetic analysis has been deposited in MorphoBank (http://morphobank.org/permalink/?P2799).

Field-specific reporting

Please select the best fit for your research. If you are not sure, read the appropriate sections before making your selection.

☒ Life sciences ☐ Behavioural & social sciences ☐ Ecological, evolutionary & environmental sciences

For a reference copy of the document with all sections, see nature.com/authors/policies/ReportingSummary-flat.pdf

Life sciences study design

All studies must disclose on these points even when the disclosure is negative.

Sample size	Our study reports the finding of a new fossil, represented by a single specimen. Comparisons with other fossils are constrained by the number of specimens that have been recovered for particular taxa; all were included where possible. Comparisons with extant mammals were conducted in the large, diverse collections of the Section of Mammals, Carnegie Museum of Natural History, Pittsburgh, USA.
Data exclusions	We sampled extinct taxa as broadly as possible, but excluded several poorly represented and poorly described fossils that we were unable to study firsthand.
Replication	We built a taxon-character matrix from scratch rather than relying on prior published matrices. The authors worked together in scoring taxa, which meant the data were internally verified.
Randomization	Our study only reports a single specimen; no randomizations were used.
Blinding	Not applicable to palaeontology.

Reporting for specific materials, systems and methods

Materials & experimental systems

n/a	Involved in the study
☒	☐ Unique biological materials
☒	☐ Antibodies
☒	☐ Eukaryotic cell lines
☐	☒ Palaeontology
☒	☐ Animals and other organisms
☒	☐ Human research participants

Methods

n/a	Involved in the study
☒	☐ ChIP-seq
☒	☐ Flow cytometry
☒	☐ MRI-based neuroimaging

Palaeontology

Specimen provenance	The specimens were collected from the Lower Cretaceous Yixian Formation at Xisanjia, Inner Mongolia, China. The collection permits were obtained from the Department of Land and Resources of China in 2008.
Specimen deposition	All specimens of this study have been deposited at the Tianyu Museum of Nature, which is accessible to other researchers.
Dating methods	No new dates are provided.

☐ Tick this box to confirm that the raw and calibrated dates are available in the paper or in Supplementary Information.